

# ROLE OF PRE-CRACK FORMATION AND ALKALI SILICA REACTION ON CONCRETE

Salhin Alaud\*, Gideon P.A.G. van Zijl†

Department of Civil Engineering, Stellenbosch, SOUTH AFRICA

## Abstract

An experimental study was designed to investigate the effect of mechanical cracks in concrete on ASR expansion. Concrete cubes were made from a reactive aggregate of Greywacke stone and ground granulated corex slag (GGCS) was added to half of the specimens. Half of the specimens were submerged in 1N NaOH solution at 80°C in accordance with ASTM C 1260, and the other half of the specimens were submerged in hot water at the same temperature. A wedge splitting test on the specimens was set to achieve a certain crack width after being subjected to accelerated ASR exposure and hot water. The cracked specimens were subsequently returned to their exposure conditions, and the crack widths were measured 2, 7, 14 and 28 days after they were pre-cracked, at the same positions. Test results indicated that the mechanical crack widths reduce due to ASR and thermal expansion with values that differ according to the initial crack widths and the binder composition.

**KEYWORDS:** Crack formation, crack width, wedge splitting, alkali-silica reaction, combined action.

## 1 INTRODUCTION

Alkali-silica reaction (ASR) is certain forms of silica in aggregates reacting in high alkaline pore solutions in concrete and presence of moisture to form a reaction product that expands and may result in cracking. Although knowledge of ASR has been increasing for several decades, the number of existing structures exhibiting ASR deterioration is apparently increasing. Extensive cracking has been found in several bridges in many countries in recent years. ASR is not the only major source of deterioration and cracking in concrete, and other causes of cracks include mechanical load, corrosion, and shrinkage. These cracks may lead to many problems such as reduced resistance to the ingress of gas, water, and deleterious matter which in turn potentially accelerate the ASR process, and also carbonation, corrosion, and other deterioration processes. Most studies have concentrated separately on the effects of mechanical loading or environmental action and not on their combined effects, despite the fact that they occur at the same time and may interact. However, a structure's serviceability and durability cannot be determined accurately without studying the combination of these actions on concrete. Ideally, a new design method is required that can account for not only the mechanical life but also the changes in properties over time due to ASR.

In this paper, the design and results are described of experiments on concrete cubes, half of them subjected to ASR exposure, and the other half submerged in hot water. Subsequently the specimens were subjected to wedge splitting to obtain specific crack widths and returned to their exposure. The ASR exposure was immersion of the samples in NaOH in a new device developed to conform to ASTM C 1260 [1] conditions. In the device, the temperature of the solution is 80 °C and the concentration of NaOH is one molar (40g of NaOH per liter). The ASTM 1260 test uses a mortar bar while plain concrete prisms were used in this experimental setup.

## 2 WEDGE SPLITTING AND ASR

The purpose of this experiment is to determine whether mechanical cracks play a significant role in ASR, and in particular whether the (initial) crack width is of importance. Experimental tests based on creation of specific mechanical cracks in concrete cubes and subjecting them to accelerated ASR conditions according to ASTM C 1260 were performed. For determining the role of temperature in crack formation and volume changes, the same experimental was carried out on cubes subjected to hot water at the same ASR temperature.

---

\* Correspondence to: [alaud@sun.ac.za](mailto:alaud@sun.ac.za)\*, [gvanzijl@sun.ac.za](mailto:gvanzijl@sun.ac.za)†

## 2.1 Materials

A Pretoria Portland Cement (PPC) type CEM I 52.5N was used. Two mixes were cast with Greywacke aggregates and Philippi sand; the first with cement CEM I only and the second with 50% of the CEM I replaced by ground granular corex slagment (GGCS). The mix proportions, by weight of cement, are shown in Table 1. The coarse aggregate gradation was: 1/3 of size 13-19 mm, 1/3 of size 9.5-13 mm and 1/3 of size 4.75-9.5 mm. The slump test result was equal to 55 mm for both mixes.

## 2.2 Test specimens and devices

Cubes of concrete with side lengths of 100 mm were used for this experimental. To prepare the samples for the test, a slot of 30 mm wide and 20 mm deep was made along the top side of the cubes. In order to ensure that crack formation will occur in the middle of a cube, a notch was made along the central length of the slot of 30 mm deep and 3 mm wide. Figure 1 illustrates the shape, dimensions and a photo of the specimens. The samples are denoted as follows: Gw/A, Gw/w, Gw-co/A and Gw-co/w (Gw = Greywacke, co = Corex Slag, w = water and A = ASR). A chamber was designed to immerse the specimens in the NaOH (part 1) and in hot water (part 2) as illustrated in Figure 2. The Instron MTM was used to perform the wedge splitting test, and to record the loading applied. Two LVDTs were set on the two sides of the specimens to measure the deformation containing the crack, and for crack mouth opening control of the test. To subsequently accurately measure the crack widths, high-resolution photos were taken with the digimicro camera (dnt) of the crack on the surface. The mechanism of the test is based on a steel wedge with a sharp edge which is forced between two rollers to convert the vertical load to a horizontal load, in order to force the two edges on the upper part of the cube apart, as shown in Figure 3.

## 2.3 Test procedure

A total of 36 specimens of the two concrete mixes were cast. After the concrete was placed in the moulds, the specimens were covered by a plastic sheet to protect them from loss of moisture in the laboratory. The specimens were demoulded after 24 hours and then placed on a perspex base in the chamber (Figure 2). Half of the specimens of each mix was submerged in NaOH (part 1) and the other half was submerged in hot water (part 2).

The volume of normal water and of 1N NaOH was four times the volume of the concrete specimens. The lid of the device was sealed, and the thermostat elements switched on to obtain a temperature in both sections of 80 °C. The specimens were extracted from the device after 7 days and were prepared to apply the wedge splitting load. Controlled wedge splitting tests were performed in a closed-loop system, controlled by one of the LVDT readings, to achieve pre-selected residual crack widths in the unloaded state of nominally 0.1 mm, 0.2 mm and 0.4 mm, with 6 specimens per crack width (three to be placed in hot water and the other three in NaOH solution). The load of the Instron MTM was progressively applied until the LVDTs read the selected crack width, after which the MTM unloaded automatically. It is possible to control the crack width during the test at the position of the LVDT on the surface. Subsequently measuring the crack after removal of the specimen from the MTM was based on high resolution photos of the specimen face (front or rear side) and noting the position of measurement. The measured crack widths directly after the splitting test were considered as reference for the later measurements at the same position. The crack width was measured on both sides in two places; one at the mouth on the top and the other in the middle of the space below the notch. Figure 4 illustrates the positions of LVDT and measurements of crack widths. High resolution photos were taken with the dnt with a magnification factor 35, of the crack on the surface. After the cracks were measured, the specimens were returned to the water and accelerated ASR exposure conditions at 80°C. Then the specimens were extracted one by one from the device to image them after 1, 2 and 4 weeks. Once a specimen had been imaged, it was immediately returned to its exposure before extracting the next specimen. After the 4<sup>th</sup> week, all the specimens were left outside the chamber in the lab condition for 1 week and the photos were taken after that, i.e. 5 weeks after the pre-cracking.

## 3 RESULTS AND DISCUSSION

The results of experiments showed that the crack widths were reduced due to concrete expansion. The crack widths in the mixtures with GGCS were reduced less than those in cement only mixtures. Also the crack widths in the specimens subjected to ASR were reduced more than those immersed in hot water.

Although the wedge splitting tests were controlled to obtain specific residual crack widths ( $C_w = 0.1, 0.2$  and  $0.4$  mm), the  $C_w$  was different based on the position of measurement. Table 2 shows the distribution of number of  $C_w$  measuring in various samples (4 for each sample) until  $700 \mu\text{m}$ , with a note that, some uncontrolled readings were excluded.

### 3.1 Crack reduction

The average reduction of crack widths at various ages is shown in Figure 5 and Figure 6. The results are illustrated for both mixes (Gw and Gw-co) in the both conditions (ASR and hot water). Each graph compares the average crack widths reduction measured at the mouth of the crack (mouth) and that measured in the middle of the space under the notch (mid). Also, it can be noted that there are differences between the strains in different cases. The reduction in crack width which reflects the expansion in concrete due to ASR or heat increased dramatically in the beginning and then later increased more slowly. The maximum concrete expansions into the cracks (crack reduction) at the mids after 4 weeks were 15.1, 8.8, 8.1 and 6.5% for Gw/A, Gw/w, Gw-co/A and Gw-co/w respectively. Since the crack widths at mids are smaller than those at the mouths, it leads to more reduction, which is discussed in section 3.2. In the 5<sup>th</sup> week when all the specimens were extracted from their exposure condition chamber, the strains in all the specimens at the mid-height diminished and the mouth crack widths reduced to 12.8, 7.5, 5.7 and 4.7% respectively. The results also show that the changes for specimens subjected to ASR and thermal expansion were larger than those due to only thermal expansion.

### 3.2 Relationship between the crack width and crack reduction

It can be noted that the smaller crack widths have more reduction than the larger ones. This phenomenon might be due to self-healing according to some previous studies. The formation of calcium carbonate  $\text{CaCO}_3$  or calcium hydroxide  $\text{Ca}(\text{OH})_2$  might be necessary for self-healing to be affected and cracks may heal after some time due to continuing hydration of clinker minerals [2,3]. Nijland et al., (2007) [3] studied the results of self-healing of over 1000 of samples of concrete and masonry mortars from different structures and found that the self-healing occurs in the presence of free lime. However, autogenous healing is only effective in the presence of water and is limited to occurring in small cracks [2]. Reinhardt & Jooss, (2003)[4] developed permeability tests on high-performance concrete (HPC) cells cracked by control splitting with crack widths between  $50$  and  $200 \mu\text{m}$  and subjected to temperatures of between  $20$  and  $80^\circ\text{C}$  to study self-healing behavior. They stated that a higher temperature leads to faster self-healing and that smaller cracks heal faster than greater ones. Huan et al., (2010) [5] studied self-healing of Engineered Cementitious Composites concrete (ECC) with fly ash under cycles of wet and dry conditions. This is a fiber reinforced mortar with controlled fine cracks under tensile or flexural load. They found that ECC is an ideal material to contribute to self-healing when the crack width is less than  $100 \mu\text{m}$ . The results indicate that, the smaller crack widths decrease more than, the larger widths. Figure 7 shows an example of images for the cracks that were taken by the dnt camera at the mouth and the middle of the wedge-splitting specimens. Other images taken of Gw/A specimens number VI side 2 in Figure 8 shows an example of self-healing in a microcrack. In this figure, it can be seen that some gel has formed in the main crack (in yellow rectangular) after 1 week, while in the secondary crack, the crack disappeared in some position (red rectangular) after 4 weeks of exposure.

The difference between the initial crack width and current crack width is denoted by  $\Delta C_w$ . This change in crack width ( $\Delta C_w$ ) after 4 weeks exposure to ASR and hot water conditions is shown as percentage of the initial crack width ( $C_w$ ) for each specimen in Figure 9. In the graph, an exponential trend line is also shown, fitted to the scattered data. The curves show that the change in crack width in specimens exposed to ASR conditions is more than that in specimens submerged in hot water, and this indicates ASR expansion. Also when the corex slag is added (Gw-co), the expansion is less than that of the concrete specimen containing only CEM I (Gw).

From the previous studies and the results presented here, it is evident that two factors may assist ASR in the self-healing process and minimize the crack width. In the presence of water and high temperature, which were provided in the experiment, self-healing occurred in small crack widths.

### 3.3 Calculating the mechanical crack reduction

The expansion in the concrete due to NaOH at  $80^\circ\text{C}$  and thermal expansion leads to reduction in the mechanical pre-cracks. The total strain  $\epsilon$  is considered to be the summation of ASR strain  $\epsilon_{asr}$  and thermal expansion  $\epsilon_T$ . Therefore, the ASR strain can be determined from:

$$\varepsilon_{asr} = \varepsilon - \varepsilon_T \quad (1)$$

It can be considered that half of the total strain expands into the crack causing the crack width reduction ( $\Delta C_w$ ), and the other half expands outwards (see Figure 9 left). In this way, the ASR swelling starts to partially fill the spaces of the mechanical cracks. The mechanism of the  $\Delta C_w$  in Figure 9 (right) is represented by an exponential curve, indicating that the small cracks are faster reducing than larger crack widths. The change in crack width can be written as follows:

$$\Delta C_w = \frac{1}{2}\varepsilon l \quad (2)$$

where  $l$  is the width of the concrete sample. To determine  $\Delta C_w$ , the expansion due to hot water (80°C) is subtracted from the total strain recorded at exposure of NaOH at 80°C as follows:

$$\Delta C_{w,ASR} = \frac{1}{2}((\varepsilon_{asr} + \varepsilon_T) - \varepsilon_T)l \quad (3)$$

The total  $\Delta C_w$  recorded at the crack mouth and mid in Figure 8 are presented by exponential curves of  $Gw/A$  (left) and  $Gw-co/A$  (right) while the curves of  $Gw/w$  and  $Gw-co/w$  in the same figure represent the expansion due to hot water. The  $\Delta C_{w,ASR}$  is represented by the separation of the two curves. By subtracting the curves induced by temperature only from those induced by NaOH and temperature, the  $\Delta C_w$  induced by ASR in  $Gw$  mix is found to be represented by the expression:

$$\Delta C_w(Gw) = 4.4957e^{0.002(C_w)} \quad (4)$$

and for  $Gw-co$  mix:

$$\Delta C_w(Gw - co) = 2.9589e^{0.002(C_w)} \quad (5)$$

The results from Equations 4 and 5 are presented in Figure 10.

Note that the initial crack widths start at 50  $\mu m$  and end at 700  $\mu m$ , based on the pre-crack widths recorded, and that the subsequent exposure time was four weeks. Different exposure times might produce the same trend, i.e. in percentage small cracks will reduce more than wider cracks. In Figures 5 and 6 it is clear that the rate of change in crack width diminishes with exposure time, i.e. as the ASR extent increases and ASR affinity approaches zero.

#### 4 CONCLUSION

The combined action of wedge splitting and ASR was studied on concrete cubes. The concrete cubes were cast and pre-cracked to study the subsequent change in mechanical cracks due to ASR. Two mixes with Greywacke stone and Philippi sand were cast, the first, with cement only and the second with 50% of the cement replaced by GGCS. Wedge splitting was applied on the specimens after one week of being cast and submerged in water and NaOH at 80°C. After a specific crack had been obtained, the specimens were returned immediately to the same liquid in the device. Photos by dnt camera were taken to measure the crack widths directly after the splitting and after 7, 14 and 28 days. The specimens were then left at lab temperature and the photos were taken after 1 week. Comparison was made between the crack width change in specimens subjected to ASR and those submerged in hot water at the same temperature (80°C). Also, a comparison was made between the mixes cast with cement only ( $Gw$ ) and those blended with corex slag ( $Gw-co$ ). The results showed that the crack widths were reduced due to ASR and thermal expansion in concrete. The smaller crack widths reduce relatively more than the larger ones and this may be to an extent due to self-healing. Generally, the crack width reduction decreased due to ASR when corex slag was added to the mix.

## 5 REFERENCES

- [1] ASTM C 1260, (2007): ASTM, Standard Test Method for potential alkali reactivity of aggregates (Mortar-Bar Method, D), Annual Book of ASTM Standards, American Society for Testing and Materials.
- [2] K. Van Tittelboom and N. De Belie, (2013): Self-healing in cementitious materials-a review, vol. 6, no. 6.
- [3] T. G. Nijland, J. a Larbi, R. P. J. Van Hees, and B. Lubelli, (2007): Self-Healing Phenomena in Concretes and Masonry Mortars : a Microscopic Study,” no. April, pp. 1–9.
- [4] H. W. Reinhardt and M. Jooss, (2003:) Permeability and self-healing of cracked concrete as a function of temperature and crack width, Cem. Concr. Res., vol. 33, no. 7, pp. 981–985.
- [5] J. H. Yu, W. Chen, M. X. Yu, and Y. E. Hua, (2010): The microstructure of self-healed PVA ECC under wet and dry cycles,” Materials Research, vol. 13, no. 2. pp. 225–231.

TABLE 1: Concrete mix proportions (kg).

<i>Mix</i>	<i>Cementitious</i>		<i>Aggregate</i>		<i>Water</i>
	Cement CEM I 52.5	Corex slag	Greywacke stone	Philippi sand	
Gw	440	-	1000	815	184
Gw-co	220	220	1000	815	202

TABLE 2: Number of cracks (original, directly after pre-crack) in 100  $\mu\text{m}$  width intervals.

<i>Sample</i>	<i>Gw/A</i>		<i>Gw/w</i>		<i>Gw-co/A</i>		<i>Gw-co/w</i>	
	Mouth	Mid	Mouth	Mid	Mouth	Mid	Mouth	Mid
<100	2	1**	3*	1**	1	4*	1	2
100-200	1*	6	5	4***	3	2	3	6
200-300	3	5	1*	1*	0**	2	1*	9
300-400	7	3	1	2	3	5	3	0
400-500	1	0*	0*	2	2	3	3**	0*
500-600	1	0	1	1*	0*	1	2	0
600-700	1*	0	3	0	3	0	1	0
>700	0	0	0*	0	0*	0	0*	0
Sum	16	15	14	11	14	17	14	17
Outliers(*)	2	3	4	7	4	1	4	1
Total	18	18	18	18	18	18	18	18

\* Number of uncontrolled measurements (considered outliers and excluded).

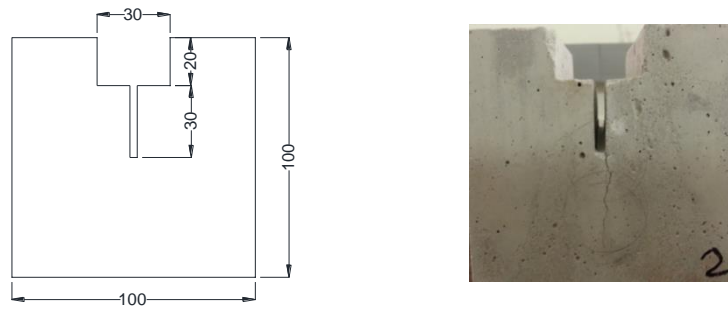


FIGURE 1: WEDGE SPLITTING SPECIMEN: DIMENSIONS (LEFT) AND PHOTO (RIGHT).

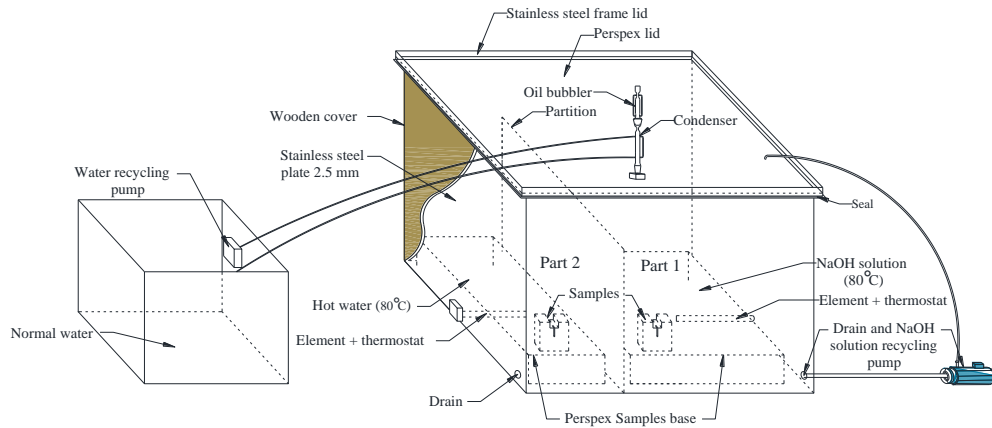


FIGURE 2: CHAMBER BUILT FOR ASR AND HOT WATER EXPOSURE.



FIGURE 3: WEDGE SPLITTING SETUP ON THE INSTRON MTM.

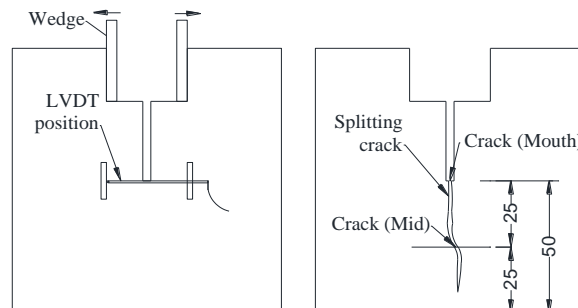


FIGURE 4: WEDGES AND LVDT POSITIONS (LEFT) AND MEASUREMENT POSITIONS OF MECHANICAL CRACK WIDTH AT MOUTH AND MID (RIGHT).

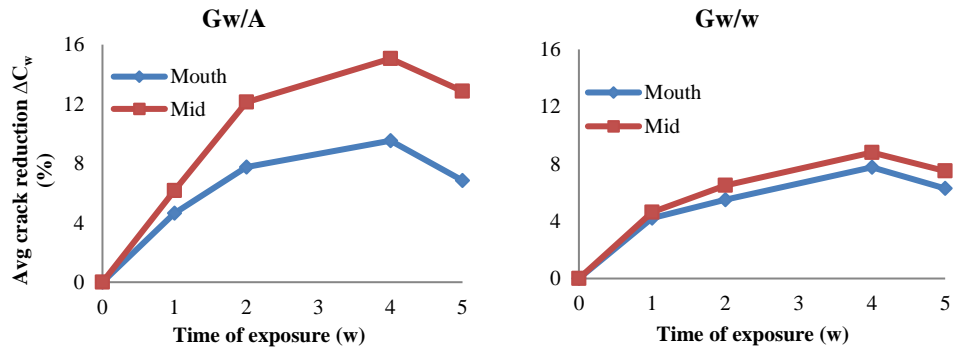


FIGURE 5: THE AVERAGE CRACK REDUCTION AS A PERCENTAGE AT 4 WEEKS OF EXPOSURE AND 1 WEEK AT LAB TEMP. FOR GW/A (LEFT) AND GW/W (RIGHT).

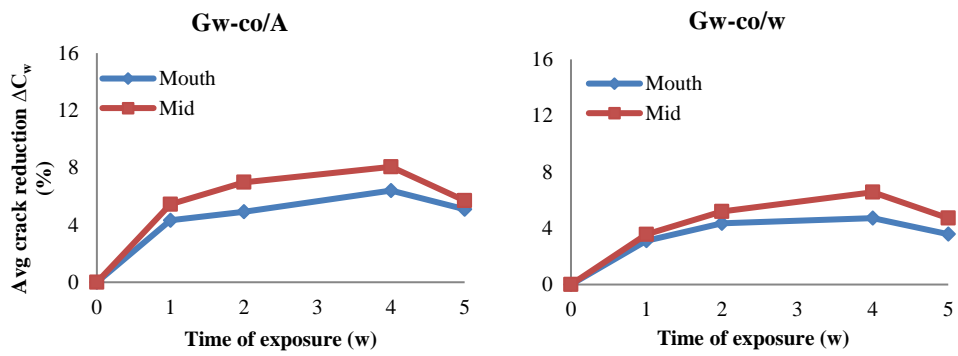


FIGURE 6: THE AVERAGE CRACK REDUCTION AS A PERCENTAGE AT 4 WEEKS OF EXPOSURE AND 1 WEEK AT LAB TEMP. FOR GW-CO/A (LEFT) AND GW-CO/W (RIGHT).

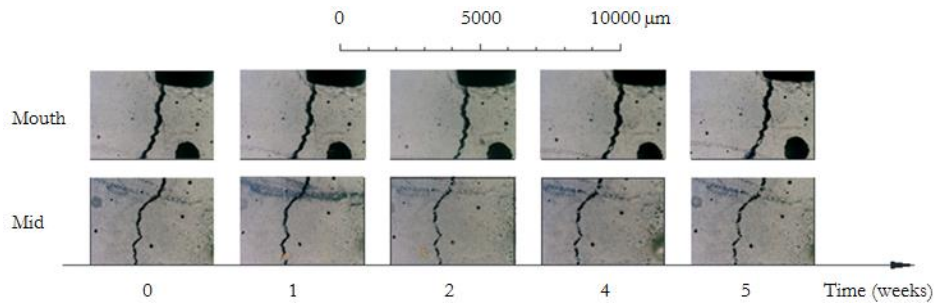


FIGURE 7: EXAMPLE IMAGES OF THE CRACKS AFFECTED BY ASR OVER THE WEEKS AT THE MOUTH AND THE MIDDLE IN GW/A SPECIMENS.

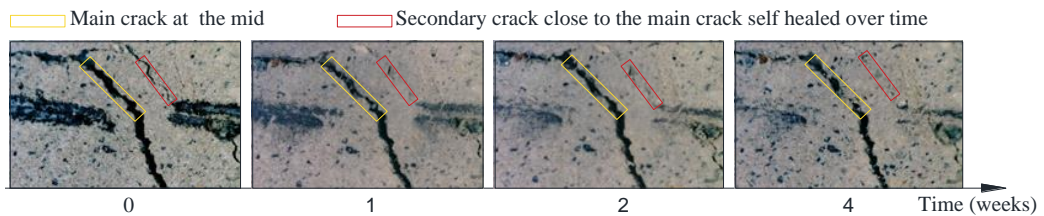


FIGURE 8: THE REDUCTION OF ALL THE CRACK WIDTHS  $\Delta C_w$  (MOUTH AND MID) VS INITIALS CRACK WIDTH DUE TO ASR AND WATER AT 80°C AFTER 4 WEEKS.

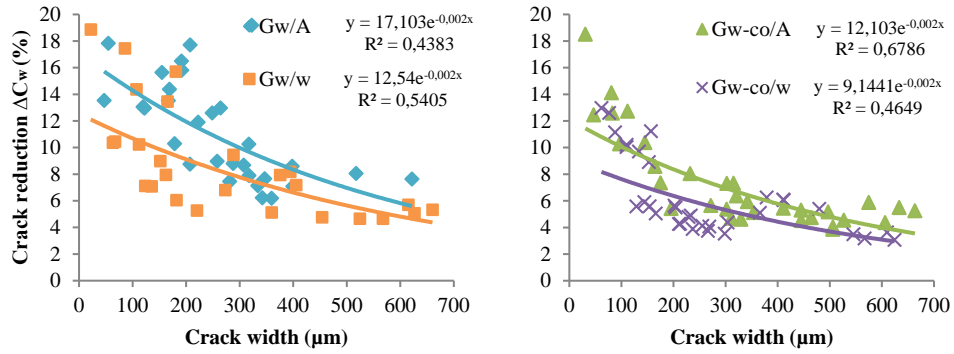


FIGURE 9: THE REDUCTION OF ALL THE CRACK WIDTHS  $\Delta C_w$  (MOUTH AND MID) VS INITIALS CRACK WIDTH DUE TO ASR AND WATER AT 80°C AFTER 4 WEEKS OF EXPOSURE: GW (LEFT) AND GW-co (RIGHT).

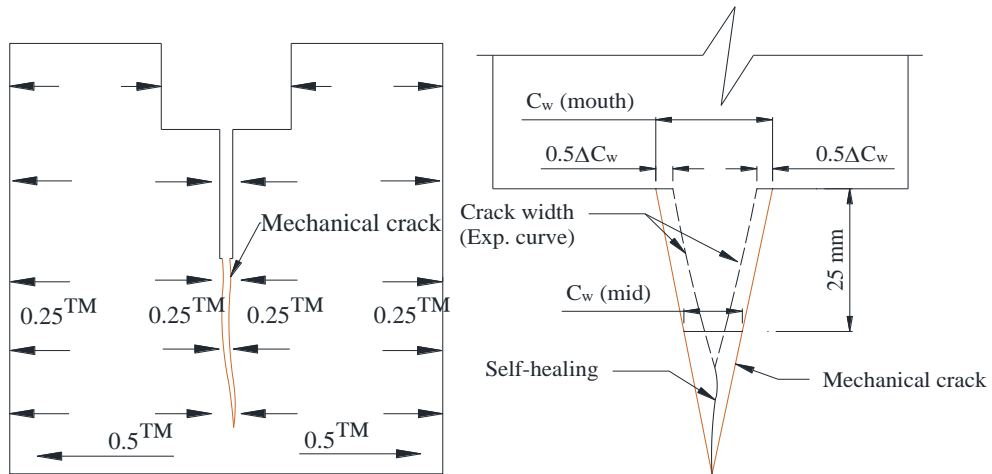


FIGURE 10: THE SUPPOSED MECHANISM OF THE CONCRETE SPECIMEN DEFORMATION DUE TO PRE-CRACKING AND ASR: DISTRIBUTION THE EXPANSIVE ASR AND THERMAL STRAIN (LEFT) AND DISTRIBUTION AND MECHANISMS OF CRACK REDUCTION (RIGHT).

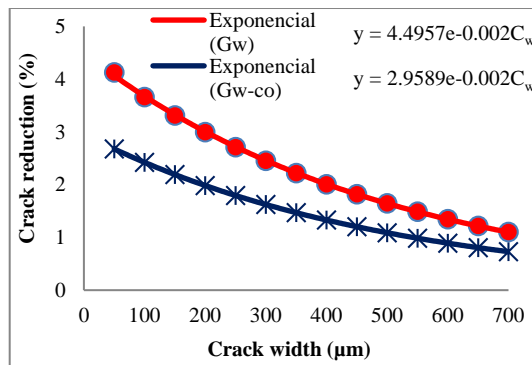


FIGURE 11: The reduction of the crack width  $\Delta C_w$  vs crack width due to ASR.